Quantum Electronics **49** (7) 698–706 (2019)

LASER MICROSCOPE https://doi.org/10.1070/QEL16724

Superresolution effect on a microstep phase image in a laser heterodyne microscope

I.M. Akhmedzhanov, D.V. Baranov, E.M. Zolotov, Yu.I. Shupletsova

Abstract. **The possibility of achieving superresolution on a microstep phase image in a laser scanning differential heterodyne microscope is studied both heoretically and experimentally. The superresolution is estimated as the width ratio for the amplitude and phase components of the microscope response measured at half the height of the corresponding parts of the response. It is shown theoretically that superresolution greatly exceeding unity can be achieved for an object in the form of a phase microstep introducing a phase shift equal to π. Superresolution of ∼2 is experimentally obtained for certified test micro-objects. A possibility of tuning a test sample into the superresolution regime by shifting a point photodetector in the microscope's Fourier plane is demonstrated.**

Keywords: *superresolution, heterodyne microscopy, phase response, phase image, microscopic object positioning.*

1. Introduction

The idea of increasing the resolution of an optical microscope using the phase component of the image optical field is well known [1, 2]. The optical phase image is defined as the optical field phase distribution in the image plane of an optical system, in contrast to the conventional image, which is defined as the optical field intensity distribution in the same plane. Currently, much interest is shown in this subject, which is apparently explained by its both fundamental and applied aspects [3, 4].

Despite a large number of publications on this subject, one cannot state that there is a unified definition of the concepts of 'resolution' and 'superresolution'. This can obviously be explained by the wide variety of methods and approaches in use, which hinder elaboration of unified definitions and call for refining the terminology in each specific case. As was noted in [1], the development of the latest microscopy methods leads, in particular, to a diffusion of boundaries between the concepts of spatial resolution and accuracy in measuring coordinates. Some researchers (see, e.g., [5]) suppose that these concepts should be distinguished; nevertheless, even they acknowledge that this cannot always be done.

I.M. Akhmedzhanov, D.V. Baranov, E.M. Zolotov Prokhorov General Physics Institute, Russian Academy of Sciences, ul. Vavilova 38, 119991 Moscow, Russia; e-mail: eldar@kapella.gpi.ru;
Yu.I. Shupletsova Institute of Legislation and Comparative Law under the Government of the Russian Federation, Bol'shaya Cheremushkinskaya ul. 34, 117218 Moscow, Russia; e-mail: ecology@izak.ru

Received 24 December 2018
Kvantovaya Elektronika **49** (7) 698–706 (2019)
Translated by Yu.P. Sin'kov

In this study we apply a generalised approach to the concept of resolution in optics [6, 7], based on estimation of the characteristic width of line spread function. Taking into account the specificity of the method in use and following [1, 8], the characteristic width of the edge response function is used as a measure of resolution. Note that this concept of resolution was already used previously, for example, in [2]. Concerning the superresolution concept, in our specific case, we consider expedient the approach proposed in [9], in which resolution is compared in the sense of accuracy in determining the range of a phase gradient maximum for a step object and the Airy disk width. Based on this approach and the definitions proposed in [7, 9], we will formulate below the definition of superresolution for the scanning differential heterodyne microscope (SDHM) used by us [10].

A possibility of forming superresolution in the SDHM was shown previously in [11, 12]. In [11] this possibility was demonstrated both theoretically and experimentally using an algorithm based on the use of *a priori* information and solving the corresponding integral equation. The specially defined superresolution parameter reached ∼3. A threefold excess of resolution above the diffraction limit was experimentally obtained in [12] when solving the inverse problem for a step object by extrapolating the SDHM response spectrum. In this context, it is of interest to analyze the possibility of forming superresolution directly based on the SDHM response, applying no additional mathematical processing and using the existing a priori information about the object. Here, step-like objects are of special interest, because the SDHM response to them has a similar bell-like shape for both the amplitude and phase components due to the specific features of the microscope optical scheme. This circumstance makes it possible to compare both components without any additional processing and introduce a quantitative parameter to estimate their width ratio. Thus, the purpose of our work was to investigate both theoretically and experimentally the complex response of the SDHM to step-like objects and demonstrate superresolution based on the analysis of the phase and amplitude response components.

The paper is organised as follows. Section 2 contains a description of the SDHM optical scheme, as well as the derivation and analysis of the analytical expressions for the response to an ideal step-like phase object. The possibility of narrowing significantly the phase response in comparison with the amplitude one is shown. The concept of resolution is considered and a quantitative criterion is introduced to characterise the revealed effect of phase response narrowing as optical superresolution. The dependence of the SDHM phase response narrowing on the parameters of the object and optical scheme is numerically investigated in Section 3. The exper-

imental results obtained on certified test objects are described and the results are discussed in Section 4. The main conclusions are formulated in Section 5.

2. SDHM optical scheme and image formation theory

The SDHM optical scheme includes a double-beam laser interferometer of the Mach–Zehnder type with a common path for both beams (Fig. 1). A He–Ne laser with a radiation wavelength $\lambda = 633$ nm is used as a radiation source. An acousto-optic modulator in the form of a Bragg cell, controlled by two harmonic signals with similar frequencies, forms two probe beams in the first diffraction order. The zero-order beam is filtered by a stop diaphragm. The diffracted beams acquire different frequency shifts in the cell and, propagating at some angle with respect to each other, are focused by a microlens (*6*) onto the surface of the object under study in two closely spaced and partially overlapping spots. The optical field intensity reflected from surface is recorded (after passing through a beam splitter) by a point photodetector located in the microlens Fourier plane. Since the Fourier plane is in the close proximity of the microlens (*6*), a lens (*5*) is used to image it in the detection plane (*9*).

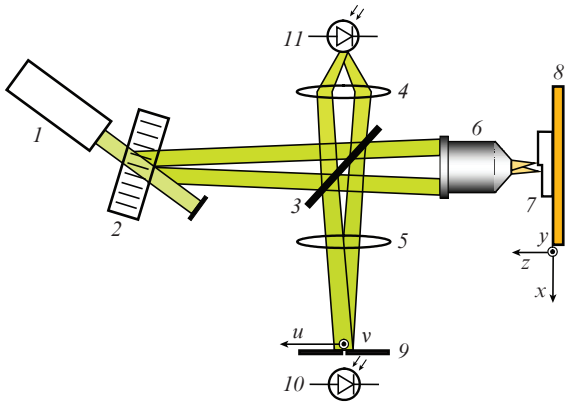

Figure 1. Optical scheme of a scanning differential heterodyne microscope: (*1*) He–Ne laser; (*2*) acousto-optic deflector (Bragg cell); (*3*) beam splitter (semitransparent mirror); (*4*, *5*) lenses; (*6*) microlens; (*7*) substrate with object; (*8*) mechanical micropositioner; (*9*) pinhole; (*10*) signal photodetector; (*11*) reference photodetector.

When probe beams with different frequencies are overlapped, a dynamic interference pattern is formed in the detection plane. The photodetector current, which is proportional to the field intensity in the detection plane, has a harmonic component at the difference frequency. The current amplitude and phase depend on the properties of the object surface. The photocurrent phase component is measured using the signal from a reference photodetector (*11*), whose phase is constant. The object is scanned along the line passing through the probe beam centres. When the object position relative to the probe beams changes, the amplitude and phase of the recorded photodetector alternating current I change as well. The functions describing the dependences of the amplitude and phase of the photodetector current on the object coordinate (i.e., the scanning coordinate x_s) will be referred to as, respectively, the SDHM amplitude and phase responses to the object under study, or, in the representation of a complex exponential function $D(x_s)$, as a complex SDHM response. The SDHM response amplitude is normalised proceeding from the condition $D(x_s) = 1$ on the unperturbed object surface.

Based on the aforesaid, the alternating current component of the photodetector, at which the light reflected from the object arrives, can be written as

$$I(x_s, t) = I_0 \mathrm{Re}\{D(x_s)\exp(\mathrm{i}\omega t)\},$$

where I_0 is the photodetector current corresponding to the reflection of radiation from the unperturbed part of the object; ω is the difference (heterodyne) frequency of probe beams; the function $D(x_s) = A(x_s)\exp[\mathrm{i}\Phi(x_s)]$ is the complex amplitude of the SDHM response; and $A(x_s)$ and $\Phi(x_s)$ are, respectively, the SDHM amplitude and phase responses. The amplitude and phase responses will also be referred to as the amplitude and phase object images in the SDHM. Concerning the experimental determination of the function $D(x_s)$, it is obvious that a measurement of the amplitude and phase of normalised current function $I(x_s, t)/I_0$ yields directly the complex response amplitude $D(x_s)$.

At the same time, when the optical scheme and object parameters are known, the complex response amplitude can be calculated either analytically or numerically, based on the theory of image formation in the SDHM. Since this theory was described in detail previously [10, 13], we present below only the key expressions that are used to model the microscope response. It is assumed that the object under study lies in the xy plane and is homogeneous along the y axis, i.e. the reflectance is independent of the coordinate y. The complex amplitude of the SDHM response for one-dimensional objects is given by the relation [10]

$$D(x_s) = L(x_s + \varepsilon/2)L^*(x_s - \varepsilon/2), \tag{1}$$

where the linear response function $L(x_s)$ is expressed in terms of the line spread function (LSF) $g(x)$ of the microscope and the local object reflectance $r(x)$,

$$L(x_s) = \int_{-\infty}^{\infty} g(x_s - x)r(x)\,\mathrm{d}x, \tag{2}$$

and ε is the distance between the centres of focused probe beams. The function $r(x)$, which determines the change in the amplitude and phase of the optical field after the reflection from the object, can be written in the form of a complex function (complex reflectance):

$$r(x) = a(x)\exp[\mathrm{i}\varphi(x)],$$

where $a(x)$ is the ratio of the amplitude moduli for the reflected and incident optical waves and $\varphi(x)$ is the change in the optical field phase as a result of reflection. The one-dimensional description of image formation is justified, because we consider here only the objects that are homogeneous along the y axis [6, 14]. A change in the phase in the reflected field may be caused, in particular, by the topographic profile of the object: $h(x)$; it this case, $\varphi(x) = 2kh(x)$, where $k = 2\pi/\lambda$. Below we consider only the phase objects for which $a(x) = 1$. The line spread function $g(x)$ is expressed in terms of the microlens pupil function $P(u, v)$ [6]:

$$g(x) = \frac{1}{2\pi}\frac{k}{f}\int_{-\infty}^{\infty} P(u,0)\exp\left(\mathrm{i}\frac{k}{f}ux\right)\mathrm{d}u.$$

Here, u and v are the linear coordinates in the microlens Fourier plane and f is the microlens focal length. It is generally assumed [6] that $P(u,v) = 1$ when $(u^2 + v^2)^{1/2} < f\mathrm{NA}$ (NA is the microlens numerical aperture) and $P(u,v) = 0$ in other cases. Then the LSF takes the form

$$g(x) = \frac{1}{2\pi}\frac{k}{f}\int_{-a}^{a}\exp\left(\mathrm{i}\frac{k}{f}ux\right)\mathrm{d}u = \frac{q_0}{\pi}\,\mathrm{sinc}(q_0 x), \tag{3}$$

where $\mathrm{sinc}(z) = \sin(z)/z$; $a = f\mathrm{NA}$ is the microlens pupil radius; and $q_0 = k\mathrm{NA}$ is the spectral half width of the spatial frequencies transmitted by the objective. Thus, relations (1)–(3) allow one to calculate the complex amplitude of the SDHM response.

Let us consider then the SDHM response to a model object, which, being an ideally reflecting phase step, provides a step phase drop φ_0 in the reflected wave. It is convenient to express the reflectance of this object in terms of the Heaviside function $H(x)$ [2]:

$$r(x) = 1 + [\exp(\mathrm{i}\varphi_0) - 1]H(x), \tag{4}$$

where $H(x) = 1$ at $x > 0$ and $H(x) = 0$ at $x < 0$. Having substituted expression (4) into (2) and then into (1), we arrive at

$$L(x_\mathrm{s}) = 1 + [\exp(\mathrm{i}\varphi_0) - 1]\tilde{H}(x_\mathrm{s}), \tag{5}$$

$$D(x_\mathrm{s}) = \{1 + [\exp(\mathrm{i}\varphi_0) - 1]\tilde{H}(x_\mathrm{s})\} \times \{1 + [\exp(-\mathrm{i}\varphi_0) - 1]\tilde{H}(x_\mathrm{s} + \varepsilon)\}, \tag{6}$$

where the function

$$\tilde{H}(x) = \frac{1}{2} + \frac{1}{\pi}\mathrm{Si}(q_0 x)$$

is expressed in terms of the integral sine function

$$\mathrm{Si}(x) = \int_0^x \frac{\sin t}{t}\mathrm{d}t.$$

Note that $\tilde{H}(-\infty) = 0$ and $\tilde{H}(+\infty) = 1$.

Since it is rather difficult to analyse expression (6) in the general form, we will consider the behaviour of the function $D(x_\mathrm{s})$ in two important cases: at $\varphi_0 \ll 1$ and at $\varphi_0 = \pi$.

In the former case the exponential can be expanded in the small parameter: $\exp(\mathrm{i}\varphi_0) = 1 + \mathrm{i}\varphi_0 - 0.5(\varphi_0)^2 + \ldots$. To represent the phase response, we leave the first two terms in this expansion and obtain as a result the expression

$$D(x_\mathrm{s}) \approx 1 + \mathrm{i}\varphi_0[\tilde{H}(x_\mathrm{s}) - \tilde{H}(x_\mathrm{s} + \varepsilon)]. \tag{7}$$

Therefore, the phase component of the response function is

$$\Phi(x_\mathrm{s}) \approx \varphi_0[\tilde{H}(x_\mathrm{s}) - \tilde{H}(x_\mathrm{s} + \varepsilon)]. \tag{8}$$

For the amplitude component, one must also take into account the quadratic term in the exponential expansion, which yields (with allowance for $\tilde{H}(x_\mathrm{s}) \approx \tilde{H}(x_\mathrm{s} + \varepsilon)$) the following relation at small ε values:

$$A(x_\mathrm{s}) \approx 1 - \varphi_0^2\tilde{H}(x_\mathrm{s})[1 - \tilde{H}(x_\mathrm{s})]. \tag{9}$$

It follows from expressions (8) and (9) that the phase response tends to zero at $\varepsilon \to 0$, i.e. when the probe beams converge. In contrast, the amplitude response does not become zero because it is not differential but is determined by the function $\tilde{H}(x_\mathrm{s})$ and the φ_0 value. At a small nonzero ε value (less than the focused beam size), both response components are bell-shaped, with lateral oscillations having a characteristic width $\Delta x = \pi/q_0$, which is determined by the coordinate of the first extremum of the integral sine. Obviously, the criterion for determining the width of the SDHM response function calls for a more correct formulation; it will be presented below.

In another important case, where $\varphi_0 = \pi$, expression (6) is reduced to the following one:

$$D(x_\mathrm{s}) = [1 - 2\tilde{H}(x_\mathrm{s})][1 - 2\tilde{H}(x_\mathrm{s} + \varepsilon)]. \tag{10}$$

Function (10) is real and alternating. It is positive everywhere, except for the interval $[0, \varepsilon]$, in which it is negative. Thus, being presented in the form of a complex exponential function, the amplitude response component is as previously a bell-shaped function with a characteristic width $\Delta x = \pi/q_0$, and the phase component is a rectangular 'pulse' with an amplitude π and a width Δx_π, equal to the distance between the points at which the functions $1 - 2\tilde{H}(x_\mathrm{s})$ and $1 - 2\tilde{H}(x_\mathrm{s} + \varepsilon)$ turn to zero, i.e., $\Delta x_\pi = \varepsilon$. Therefore, decreasing the ε value, one can reduce the phase response width by the step. This change in the response shape is due to the nonlinear character of the phase component, which was indicated for the first time in [2]. However, the analysis in that study was performed for another scheme of the phase microscope and another phase object.

Thus, we revealed that the ratio of the characteristic widths of the amplitude and phase responses may change significantly as functions of the step object characteristics. Following [8, 9], we will determine the resolution R for the SDHM as the FWHM of the response to a step object. The response height (or peak-to-peak value) is measured between the response baseline, corresponding to a homogeneous substrate surface, and the main extremum of the response function (Fig. 2). The baseline is unity and zero for the normalised amplitude response and the phase response, respectively. The physical meaning of this definition of resolution is obvious: the resolution characterises in this case the accuracy in determining the step coordinate, i.e., the coordinate of the profile point at which the modulus of its gradient is maximum. Note that this definition of resolution is not radically new [1, 6–8]; it is quite expedient in some cases, including the SDHM case.

Thus, we have two object images for the two components of the SDHM response and, correspondingly, two resolution values: amplitude (R_a) and phase (R_φ) ones. As follows from relations (8)–(10), in terms of this definition, the resolution will depend on the response component (phase or amplitude) it is measured on, as well as on the phase drop φ_0 introduced by the step.

Relations (8)–(10) are universal at $\varepsilon \to 0$, because they are determined by only the behaviour of the integral sine function and the parameter φ_0. This circumstance makes it possible to investigate the resolution according to the FWHM criterion. Numerical calculations performed with allowance for relations (8) and (9) for the SDHM response to a phase step with a drop $\varphi_0 \ll 1$ and small ε values ($\varepsilon \ll \Delta x$) yielded the following resolution values: $R_\mathrm{a} = 2.4/q_0$ for the amplitude

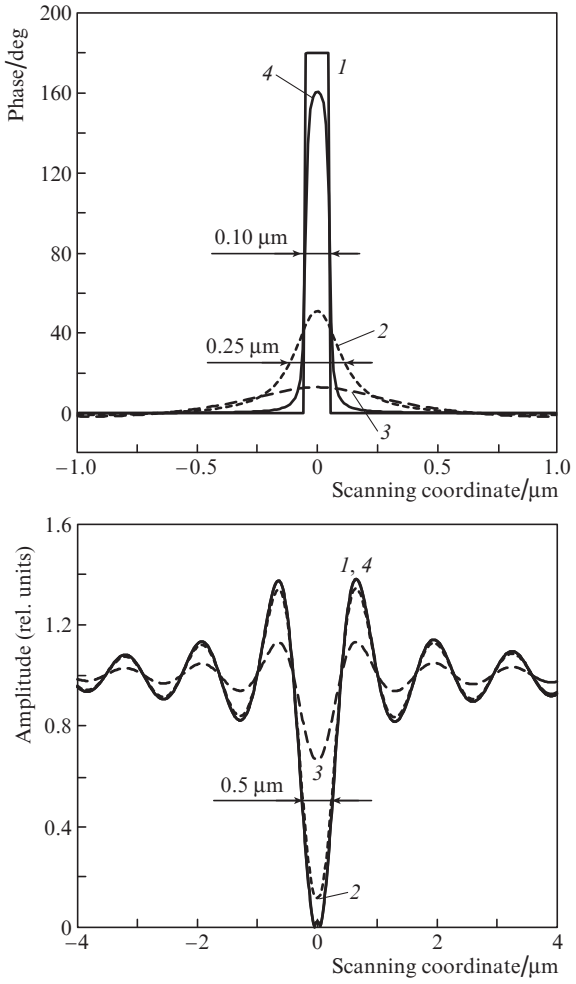

Figure 2. Calculated SDHM responses to a phase rectangular step with a height of (*1*) $\lambda/4$, (*2*) $\lambda/5$, (*3*) $\lambda/10$, and (*4*) $\lambda/3.93$, at a distance of 0.1 μm between the probe beams.

response and $R_\varphi = 3.5/q_0$ for the phase response. Note that, in correspondence with the Rayleigh criterion, the resolution is $R_I = \lambda/(2\mathrm{NA}) = \pi/q_0$ at these parameters of the system. This circumstance reflects the well-known fact that, according to the Rayleigh criterion, the resolution is equal (accurate to a coefficient of ~1) to the instrumental function width [7].

If the phase drop φ_0 introduced by a step object becomes equal to π, the situation, according to relation (10), changes radically. The resolution R_a, determined from the amplitude response, is equal as previously to $2.4/q_0$ and corresponds to the Rayleigh criterion, whereas the resolution R_φ, determined from the phase response, is ε. This means that the resolution in a phase image is determined in this case by only the distance between the probe beams in the object plane. Theoretically, one can expect for this object a significant increase in the resolution on a phase image of a microstep in the SDHM. The numerical value of resolution in the amplitude image corresponds approximately to the classical Rayleigh resolution in both cases; therefore, according to [1, 7, 9], we propose to determine in this case the quantitative parameter of superresolution SR as the ratio of the width of the instrumental function amplitude component to the phase component width:

$$\mathrm{SR} = R_a/R_\varphi, \qquad (11)$$

which yields SR ≈ 0.7 at $\varphi_0 \ll 1$ (i.e., the absence of superresolution), whereas at $\varphi_0 = \pi$ we have $\mathrm{SR} = R_a/\varepsilon$. The latter value may greatly exceed unity with a decrease in the distance ε between the probe spots. This fact indicates that superresolution may be achieved.

3. Results of numerical calculations

Let the first object be a step with a vertical wall of height h. As was noted above, at $h = \lambda/4$ (which corresponds to the introduced phase difference $\varphi_0 = 2k\lambda/4 = \pi$), the phase response has a shape of a rectangular function with a width equal to the distance ε between the centres of focused probe beams on the object surface. For example, at $\varepsilon = 0.1$ μm, the width of the calculated phase response is 0.1 μm, whereas the amplitude response width is 0.5 μm [Fig. 2, curve (*1*)]. At the points on the scanning coordinate scale, where the amplitude response is almost zero, the phase response undergoes a jump by 180°. In our case the distance between these points is ε. According to relation (11) for the aforementioned responses [Fig. 2, curves (*1*)], SR ≈ 5 at $\varepsilon = 0.1$ μm. Having reduced the ε value, for example to 0.05 μm, we obtain SR ≈ 10.

At a small deviation of the step height from $\varphi_0 = \pi$, the phase response shape starts changing: the peak-to-peak value decreases, while the response width increases. As calculations showed, with a change in the step phase drop by no more than 3° (or 0.05 rad), the phase response retains its width [Fig. 2, curve (*4*)]. If the step height differs significantly from $\lambda/4$, the phase response broadens, as well as the amplitude response [curve (*3*)]. However, even at a step height of $\lambda/5$, which corresponds to an introduced phase difference of 144°, the effect of phase response narrowing is retained [Fig. 2, curve (*2*)] and, according to formula (11), allows one to reach a twofold superresolution.

The behaviour of the SDHM phase and amplitude responses with a change in the distance ε between the probe beams is radically different (Fig. 3). It can be seen that, at a step height of $\lambda/4$, the phase response width is directly proportional to ε, whereas the amplitude response width increases by only ~50% with an increase in the parameter ε by a factor of five.

Similar regularities are also observed for a phase step whose wall is not vertical but makes some angle with the normal. In this case an increase in the step width w (see Fig. 5) at a fixed height of $\lambda/4$ leads to a decrease in the phase peak-to-peak value and phase response broadening [Fig. 4, curves (*2–4*)]. However, even at a step width of $w = 0.3$ μm, the superresolution is retained and reaches ~2 [curve (*4*)]. In this case, there is height (slightly differing from $\lambda/4$) for a tilted-wall step at which the phase response has also a rectangular shape [curve (*5*)]. Note that all amplitude responses in Fig. 4 have an approximately identical shape and width; they are not enumerated for this reason. An increase in the step width only slightly reduces the peak-to-peak value for the amplitude response.

Thus, we can conclude that the effect of interest is not critical to deviation of one of the step parameters from desired, because this deviation can be compensated for by changing another parameter. Due to this, one would expect the effect to be experimentally observed. To this end, we used certified test samples [15], which are applied to calibrate scanning optical and electron microscopes. The application of certified samples is especially important from the point of view of further study of the effect. Two types of test samples were

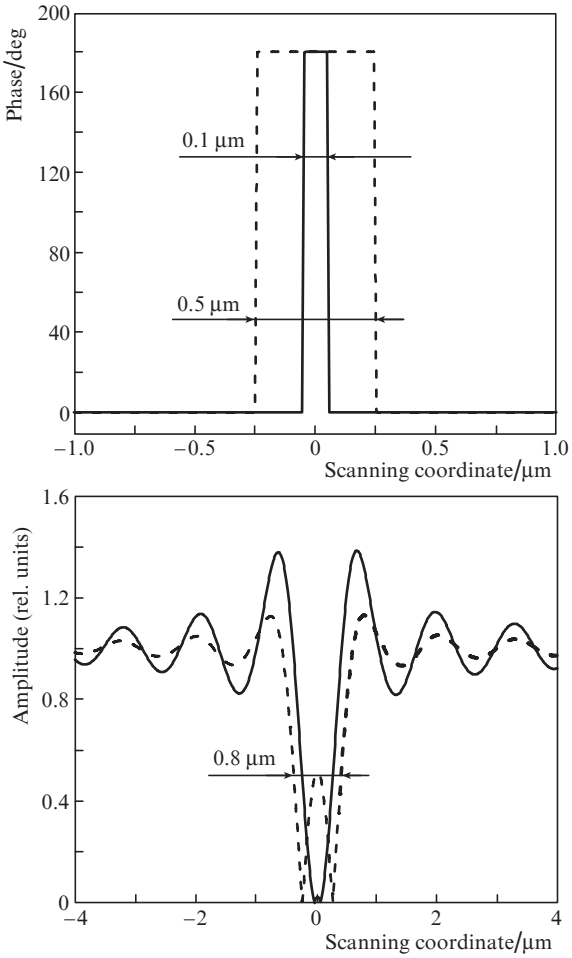

Figure 3. Calculated SDHM responses to a phase rectangular step with a height of $\lambda/4$, at distances of 0.1 μm (solid line) and 0.5 μm (dashed line) between the probe beams.

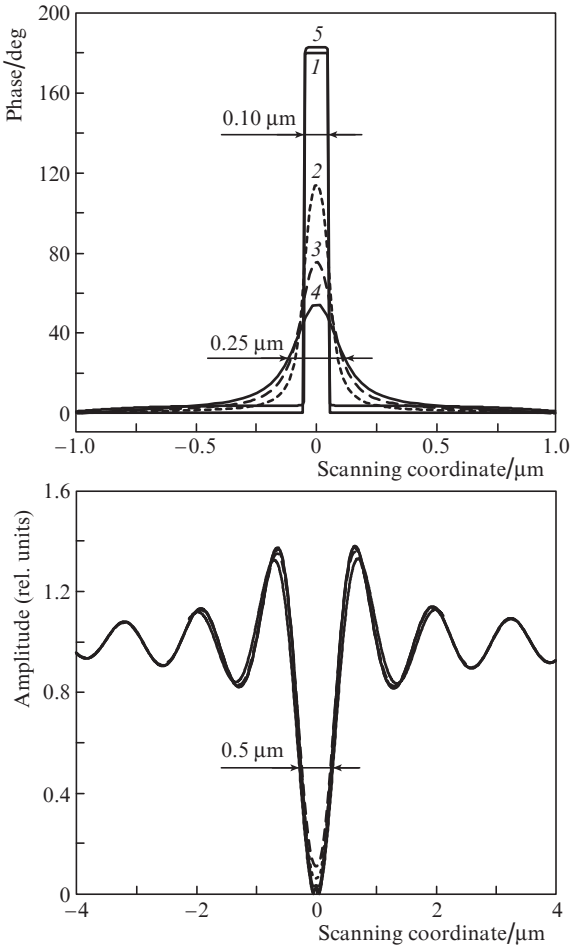

Figure 4. Calculated SDHM responses to different phase steps: (*1*) a step with a height of $\lambda/4$ and a rectangular profile; (2–4) a step with a height of $\lambda/4$ and a tilted wall with widths w = (*2*) 0.1, (*3*) 0.2, and (*4*) 0.3 μm; and (*5*) a step with a height of $\lambda/3.2$ and width w = 0.3 μm. The distance between the probe beams is 0.1 μm.

investigated: dielectric and metallised steps (Fig. 5). The metallised sample is a phase step with a constant modulus of reflectance, whereas the dielectric sample is an amplitude–phase step with a coordinate-dependent reflectance modulus.

Before carrying out the experiment, we simulated numerically the complex SDHM response for an amplitude–phase step. The simulated dependences (Fig. 6) show that a rectangular phase response can also be obtained for this object; however, the corresponding step height will differ from $\lambda/4$. This can be explained by the influence of interference in the dielectric film; thus, the necessary change in the height will depend on not only the geometric parameters but also on the refractive indices of the substrate and film. As well as for a phase step, the wall tilt can also be compensated for in this case by changing the step height [curve (*3*)] to form a phase response of rectangular shape. Thus, the numerical simulation results give grounds to verify experimentally the superresolution effect on a phase microstep image in the SDHM.

4. Experimental results

Two types of certified objects were experimentally investigated to verify experimentally the effect of superresolution on a phase image in the SDHM. The first object was an edge of a

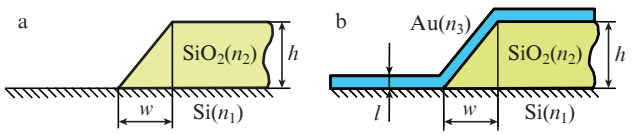

Figure 5. Schematic profiles of the experimentally studied (a) dielectric and (b) metallised step-like objects. The profile parameters are as follows: height h = 0.35 μm, wall width w = 0.30 μm, metal-layer thickness l = 25 nm, n_1 = 3.9 −0.2i, n_2 = 1.48, and n_3 = 0.16 −3.2i.

silicon dioxide film on a silicon substrate (Fig. 5a) [15]. The film thickness was 356 ± 1 nm, and the edge tilt angle with respect to the surface normal was 40°. This angle was formed by film isotropic etching. The second object was the same film edge but coated (jointly with the substrate) with a 25-nm-thick gold layer (Figs 5b). The SDHM was used to scan the profiles of both objects in the standard signal detection regime (point photodetector located at the centre of the Fourier plane). The radius of the microscope probe beam on the object surface was 0.7 μm [16]. The SDHM responses to these steps, obtained with a microlens having a numerical aperture NA = 0.65, are shown in Fig. 7.

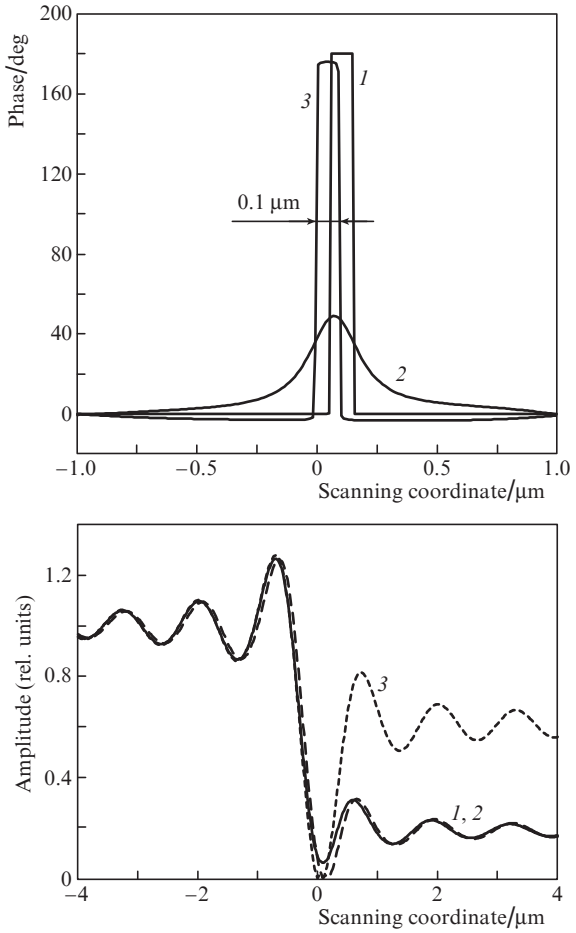

Figure 6. Calculated SDHM responses to different amplitude–phase steps: (*1*) a step with a height of $\lambda/2$ and a rectangular profile, (*2*) a step with a height of $\lambda/2$ and a tilted wall 0.3 μm wide, and (*3*) a step with a height of $\lambda/1.7$ and a projection of 0.3 μm. The distance between the probe beams is 0.1 μm.

Estimation of the resolution from the response width at half maximum for the phase and amplitude components yields (see Fig. 7) the following values of the superresolution parameter: SR ≈ 1.4 for the metallised step and SR ≈ 2.3 for the dielectric step. Note that the samples studied were not optimised previously in any way to analyse the superresolution effect, i.e. the phase drop φ_0 introduced by the step objects under consideration differed significantly from π.

Based on the results obtained, we can conclude that the resolution increases on the phase image in the SDHM and that superresolution can be achieved for a certain class of objects. Obviously, the question of practical application of this effect calls for separate investigations. In this study we consider only two aspects important from this point of view: (i) the influence of noise on this effect and (ii) the possibility of its adjustment using microscope tools.

A detail analysis of all noise sources and their influence on the results of measuring the response was beyond the scope of our study. We restricted ourselves to the estimation of the summary effect of all experimental noises on the final result of measuring the complex SDHM response, which manifests itself in the spread of individual measurement results when scanning an object. To estimate the noise influence, we performed multiple scanning of the object. This approach allowed us to construct responses taking into account the influence of the spread of individual measurements. The thus obtained SDHM responses are presented in Fig. 8. Based on the averaged phase and amplitude responses with a spread at each scanning point, one can conclude that the influence of noise on the SDHM response must be taken into consideration; however, it is obvious that the effect of phase response narrowing is retained even when taking the noise into account.

The width of measured responses was estimated by calculating the moments of the function $f(x)$ [17]. First the coordinate $x_0 = m_1/m_0$ and then the variance $\sigma^2 = m_2/m_0 - x_0^2$ were determined. Here, m_n ($n = 0, 1, 2$) are the moments of the function $f(x)$, found from the formula

$$m_n = \int_{x_1}^{x_2} x^n f(x)\,\mathrm{d}x. \qquad (12)$$

In this case, the 2σ was taken to be the width of the function. When calculating the moments of the function, integration in expression (12) was performed within the central part of the response: $x_1 = 9.5$ μm and $x_2 = 11.0$ μm. A calculation of the function width with allowance for the statistics yielded the following values: $2\sigma = 0.30–0.45$ and $0.70–0.90$ μm for the phase and amplitude responses, respectively. As a result, the superresolution parameter SR for the SDHM was estimated to be in the range of 1.5–3.0.

Concerning the possibility of increasing resolution for the samples that were not optimised with respect to the introduced phase drop φ_0 that differed significantly from π, it was experimentally found that an important parameter of the SDHM optical scheme, which allows one to adjust resolution, is the coordinate of the point photodetector in the microscope Fourier plane. In the standard measurement mode the photodetector is placed at the centre of the plane, and the microscope bandwidth is determined by the microlens numerical aperture. When the photodetector is displaced from the centre, the spatial frequency bandwidth is expanded due to the detection of the optical field spatial frequencies diffracting at an angle exceeding the aperture angle. Previously this technique was applied to enhance the microscope sensitivity [18]; however, the increase in the resolution was not studied. We investigated the dependence of the shape of the SDHM phase response to a metallised step on the photodetector displacement. The experimental responses are presented in Fig. 9 as functions of the angular coordinate of the detector. The linear coordinate u in the Fourier plane was transformed into an angular coordinate according to the formula $\theta = \arctan(u/f)$, where $f = 4.3$ mm is the objective focal length. Since a step-like object is asymmetric, the change in the response is different for the photodetector displacements to different sides from the centre ($\theta = 0$). At one side from centre ($\theta < 0$) the phase response broadens and decreases in peak value. At the other side ($\theta > 0$) it increases in peak value and narrows, reaching limiting values at a certain point of the Fourier plane ($\theta = 11°$). For the object under study, the smallest response width at this point is 0.5 μm; i.e., it is smaller by a factor of 1.6 than the result of measuring at the centre of the Fourier plane. In this case the superresolution parameter is SR ≈ 2.4.

We should note again that the effect of increasing resolution and achieving superresolution for certain classes of step-like microscopic objects via phase image analysis was thoroughly investigated for the first time in [2], where it was emphasised that the effect is based on the phase response nonlinearity and must always be correctly interpreted. In contrast to [2], we showed that the implementation of this effect does

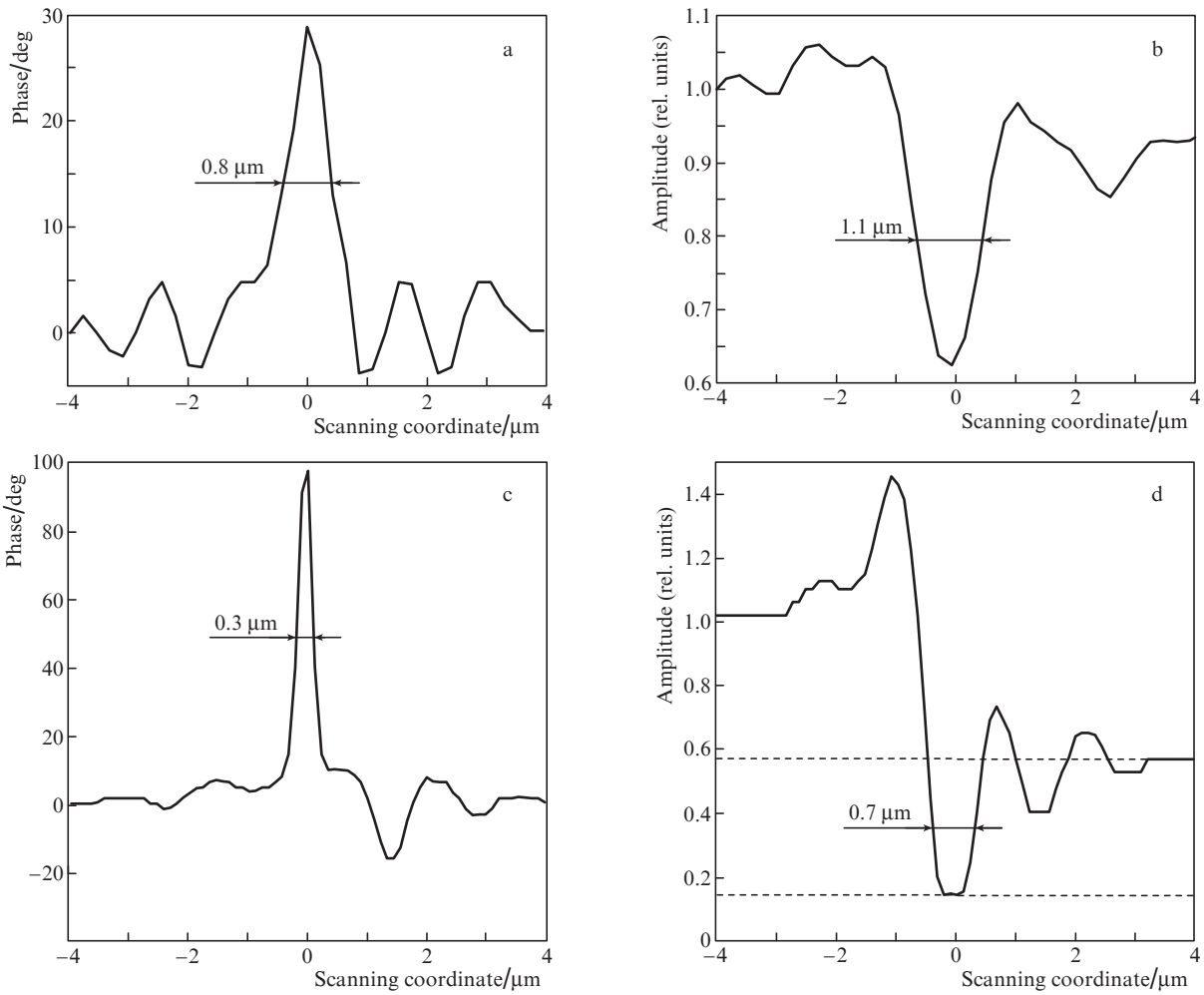

Figure 7. Experimental SDHM responses to (a, b) metallised and (c, d) dielectric steps; the distance between the probe beams is 0.3 μm.

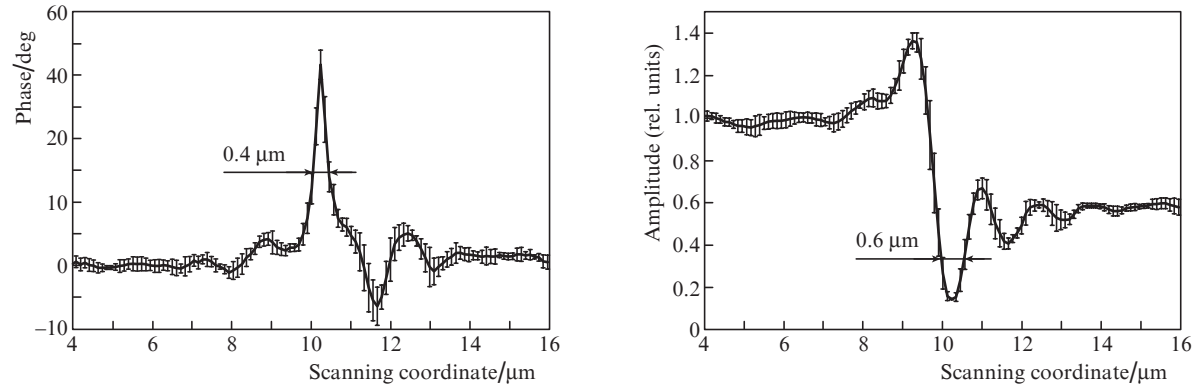

Figure 8. Experimental SDHM response to a dielectric step with allowance for statistical measurements, at a distance of 0.2 μm between the probe beams.

not require the amplitude response to pass through zero and that the superresolution parameter exceeds 2 when the phase difference introduced by the object lies in the range of 140°–180°. The manifestation of this effect in scanning differential heterodyne microscopy, which was considered in this work, appears especially promising for practical applications (e.g., for designing precise coordinate sensors in positioning devices). Therefore, it is of undoubted interest for further study.

5. Conclusions

Based on the above presented and discussed results, we can draw the following main conclusions:

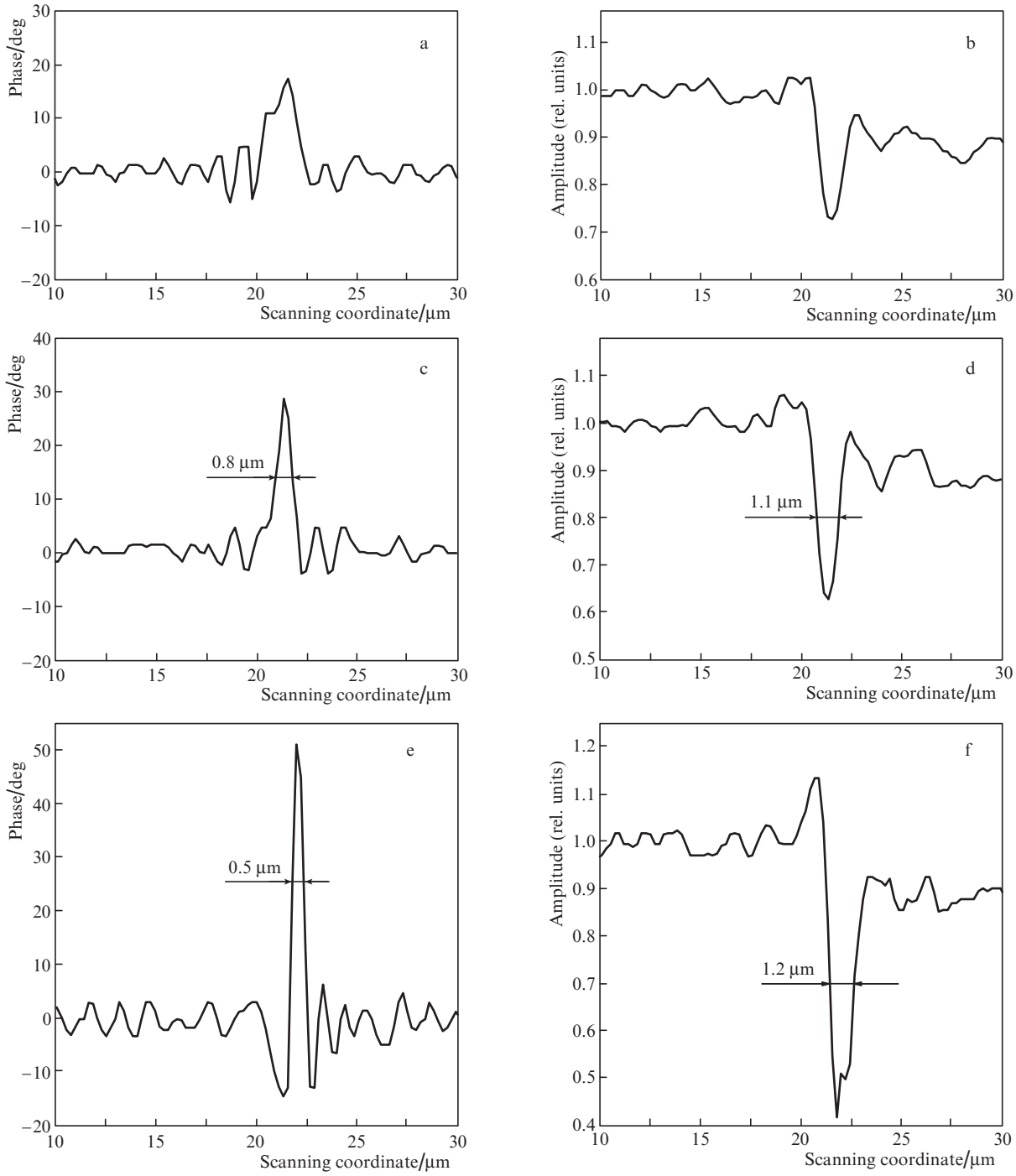

Figure 9. Experimental SDHM response to a metallised step at a distance of $\varepsilon = 0.3$ μm between the probe beams and different values of the angular photodetector coordinate in the Fourier plane: θ = (a, b) –5°, (c, d) 0, and (e, f) 11°.

1. The complex response of a scanning differential heterodyne microscope to submicron step-like phase and amplitude–phase objects was theoretically and experimentally investigated.

2. The possibility of controlling the phase response width and achieving superresolution by changing the distance between the SDHM probe beams and displacing the photodetector in the Fourier plane is demonstrated.

3. The experimental value of the superresolution parameter for certified test microscopic objects, obtained on the phase image of a step microscopic object, turned out to be ~2.

References

1. Tychinskii V.P. *Phys. Usp*., **51**, 1161 (2008) [*Usp. Fiz. Nauk*, **178**, 1205 (2008)].
2. Totzeck M., Krumbuegel M.A. *Opt. Commun*., **112**, 189 (1994).
3. Paur M., Stoklasa B., Hradil Z., Sanchez-Soto L.L., Rehacek J. *Optica*, **3**, 1144 (2016).
4. Tham W.K., Ferretti H., Steinberg A.M. *Phys. Rev. Lett*., **118**, 070801 (2017).
5. Novotny L., Hecht B. *Principles of Nano-optics* (Cambridge: Cambridge University Press, 2006) p. 89.
6. Wilson T., Sheppard C.J.R. *Theory and Practice of Scanning Optical Microscopy* (London: Academic Press, 1984).

7. Kosarev E.L. *Metody obrabotki eksperimental'nykh dannykh* (Methods for Processing Experimental Data) (Moscow: Fizmatlit, 2008) pp 68, 104.
8. Smith S.W. *The Scientist and Engineer's Guide to Digital Signal Processing* (San Diego, CA: California Technical Publ., 1999) p. 423.
9. Kretushev A.V., Tychinskii V.P. *Quantum Electron*., **32**, 66 (2002) [*Kvantovaya Elektron*., **32**, 66 (2002)].
10. Akhmedzhanov I.M., Baranov D.V., Zolotov E.M. *J. Opt. A*, **5**, S200 (2003).
11. Bozhevol'naya E.A., Bozhevol'nyi S.I., Zolotov E.M., Postnikov A.V., Rad'ko P.S. *Sov. J. Quantum Electron*., **22**, 344 (1992) [*Kvantovaya Elektron*., **19**, 379 (1992)].
12. Baranov D.V., Egorov A.A., Zolotov E.M., Svidzinskii K.K. *Opt. Spectrosc*., **88**, 466 (2000) [*Opt. Spektrosk*., **88**, 519 (2000)].
13. Akhmedzhanov I.M., Baranov D.V., Zolotov E.M. *Laser Phys*., **24**, 085901 (2014).
14. Aguilar J.F., Mendez E.R. *J. Opt. Soc. Am. A*, **11**, 155 (1994).
15. Volk Ch.P., Gornev E.S., Novikov Yu.A., Ozerin Yu.V., Plotnikov Yu.I., Prokhorov A.M., Rakov A.V. *Mikroelektron*., **31**, 243 (2002).
16. Akhmedzhanov I.M., Baranov D.V., Zolotov E.M. *Opt. Spectrosc*., **108**, 656 (2010) [*Opt. Spektrosk*., **108**, 696 (2010)].
17. Papoulis A. *Systems and Transforms with Applications in Optics* (New York: McGraw-Hill, 1968; Moscow, Mir, 1971).
18. Akhmedzhanov I.M., Baranov D.V., Zolotov E.M. *Tezisy dokladov XLI Vserossiiskoi konf. po problemam matematiki, informatiki, and fiziki i khimii* (Proc. XLI All-Russia Conf. on the Problems of Mathematics, Informatics, Physics, and Chemistry) (Moscow: Peoples' Friendship University of Russia, 2005) p. 130.